Original Research

A novel compressive stress-based osteoarthritis-like chondrocyte system

In-Chi Young[1], Sung-Ting Chuang[2], Amit Gefen[3], Wei-Ting Kuo[1], Chun-Ting Yang[1], Chia-Hsien Hsu[4] and Feng-Huei Lin[1]

[1]Institute of Biomedical Engineering, National Taiwan University, Taipei 10672, Taiwan; [2]Institute of Pharmacology, College of Medicine, National Taiwan University, Taipei 10051, Taiwan; [3]Department of Biomedical Engineering, Tel Aviv University, Ramat Aviv 69978, Israel; [4]Institute of Biomedical Engineering and Nanomedicine, National Health Research Institute, Miaoli 35053, Taiwan
Corresponding authors: Feng-Huei Lin. Email: double@ntu.edu.tw; Chia-Hsien Hsu. Email: chsu@nhri.org.tw

Impact statement

The lack of an effective treatment for osteoarthritis (OA) reflects the great need for alternative therapies and drug discovery. Disease models can be used for early-stage compound screening and disease studies. Chondrocytes are solely responsible for the maintenance of the articular cartilage extracellular matrix. Our strategy involved the generation of a cell-based model of OA, a more readily studied disease. Instead of using animal cartilage explants, we incorporated isolated porcine chondrocytes with hydrogel to form three-dimensional assemblies. We could identify the specific magnitude-dependent metabolic responses of chondrocytes by applying a series of static and cyclic compression, and therefore successfully generated a novel OA-like cell-based model for drug screening.

Abstract

Mechanical stress damage and insufficient self-repair can contribute to osteoarthritis (OA) in the affected joint. As the effects of stress on chondrocyte metabolism can regulate cartilage homeostasis, the specific stress–response condition is therefore a key to the generation of an OA disease model. We aimed to produce a specific stress- and cell-based OA model after evaluating the metabolic responses of chondrocytes in response to a series of static and cyclic compression stressors. A static load exceeding 40 psi initiated extracellular matrix (ECM) degradation through a decrease in the sulphated-glycosaminoglycan (GAG) content, upregulation of catabolic matrix metalloproteinase (MMP)-13 encoding gene expression, and downregulation of the ECM-related aggrecan and type II collagen encoding genes within 24 h. Indicators of pro-inflammatory events and oxidative stress were found to correlate with increased IL-6 expression and reactive oxygen species (ROS) production, respectively. However, chondrocytes stimulated by moderate cyclic loading (30–40 psi) exhibited increased ECM-related gene expression without significant changes in catabolic and pro-inflammatory gene expression. BMP-7 expression increased at cyclic loading levels above 30–60 psi. These results demonstrated that static compression exceeding 60 psi is sufficient to produce OA-like chondrocytes that exhibit signs of ECM degradation and inflammation. These OA-like chondrocytes could therefore be used as a novel cell-based drug screening system.

Keywords: Chondrocyte, osteoarthritis, compressive stress, static loading, cyclic loading, biomedical

***Experimental Biology and Medicine* 2017; 242: 1062–1071. DOI: 10.1177/1535370217699534**

Introduction

Osteoarthritis (OA) is a degenerative joint disease associated with defects in the integrity of the articular cartilage and related changes to the subchondral bone, ligaments, periarticular muscles, and synovium.[1] OA is the most common form of arthritis and a leading cause of disability in people older than 65 years.[2] Alterations in local mechanical factors, such as traumatic injury, bone malalignment, ligament instability, or excessive weight bearing, have been associated with OA.[3]

During the progression of OA, joint damage from mechanical stress combined with insufficient self-repair can contribute to the disease; specifically, a shift in the chondrocyte phenotype in response to an altered load yields an extracellular matrix (ECM) that cannot support normal joint function.[4–6] Here, the levels of type I collagen and denatured type II collagen increase in the ECM, whereas the levels of glycosaminoglycans (GAGs) decrease consequent to the activation of matrix-degrading enzymes. This process disrupts the balance between anabolic and catabolic metabolism in the ECM.[7,8] In addition, excessive mechanical stress was shown to increase the production of reactive oxygen species (ROS), which can lead to the hyaluronic acid depolymerization or even chondrocyte death that are apparent in OA cartilage.[9–12] Currently, OA therapy involves primarily conservative treatments, including muscle-strengthening

exercises and analgesics; if ineffective, these may be followed by osteotomy or joint replacement.[6,13] These surgical interventions, however, cannot totally restore or repair the biomechanical functions of the degenerative cartilage.[14] The lack of an effective treatment for OA has placed a heavy economic burden on healthcare systems and reflects the great need for alternative therapies and drug discovery. *In vitro* cell-based systems are therefore emerging as useful disease models for the early-stage screening of potential compounds.[15]

Cell-based OA systems can be classified by induction method, examples of which include mechanically induced cartilage trauma, enzymatically induced ECM damage, and chondrocyte metabolism dysregulation induced by substances such as mono-iodoacetate, collagenase, IL-1β, and papain.[16–20] Because articular cartilage is a weight-bearing tissue in many joints, we believe that mechanical stress-induced OA systems represent the factors that contribute to OA in weight-bearing joints.

Mechanical loading can be classified as static and cyclic, depending on frequency.[21] Many studies of cartilage tissue explants have demonstrated that the responses of developing tissues depend on the loading profile (e.g. static vs. cyclic).[22] Although the mechanisms by which mechanical stresses affect chondrocytes are not fully understood, the loading magnitude and type may be key influences on OA induction. Therefore, this study aimed to evaluate the metabolic responses of chondrocytes and thus produce an OA-like chondrocyte-based system using a specific loading condition. We applied mechanical compressive stress to primary porcine articular chondrocytes using a series of cyclic and static compression loading magnitudes. We analyzed the expression of selected ECM-related (type I collagen, type II collagen, and aggrecan) catabolic (MMP-13), anti-catabolic (TIMP-1), pro-inflammatory (IL-6), and anabolic (TGF-β_1) genes to examine the effects of compressive stress on chondrocyte gene expression. Further, we evaluated BMP-7 protein expression, ROS production, and sulphated GAG levels to assess the impact of compressive stress on stimulated chondrocytes.

Materials and methods

Chondrocyte isolation

Porcine chondrocytes were isolated from the macroscopically normal cartilage of pig femoral condyles.[23] Finely diced cartilage pieces were incubated in phosphate-buffered saline (PBS) containing a 10% antibiotic solution (15240-062; Gibco, Gaithersburg, MD, USA) at 37°C for 10 min and resuspended in Dulbecco's modified Eagle's medium (DMEM, D5648; Sigma, St. Louis, MO, USA) containing 10% fetal bovine serum (12003C; SAFC, Sigma), 1% penicillin, 0.05% L-ascorbic acid (A5960; Sigma), and 0.2% collagenase (C0130, Sigma) at 37°C for 18 h. Chondrocytes were subsequently collected and cultured in DMEM.

Preparation of a thermosensitive chitosan/gelatin/β-GP (C/G/GP) hydrogel cell carrier

C/G/GP hydrogel was previously used as a cell carrier for the nucleus pulposus and was shown to provide a uniform three-dimensional (3D) structure for cell proliferation.[24] This hydrogel was generated by dissolving 2.5% chitosan (448877, Sigma) and 1% gelatin (G2625, Sigma) in 0.1 M acetic acid (242853, Sigma), followed by autoclave sterilization. Next, a 44.4% glycerol 2-phosphate disodium salt hydrate (β-GP, G6251, Sigma) solution was filter-sterilized using a 0.22-μm filter (Millex-GV; Merck Millipore, Billerica, MA, USA) and added to the chitosan/gelatin solution dropwise while stirring.

Preparation of the polydimethylsiloxane membrane

The polydimethylsiloxane (PDMS) membrane was prepared using a silicone elastomer kit (Sylgard 184; Dow Corning, Midland, MI, USA). The pre-polymer and curing agent were mixed at the recommended ratio of 10:1 to yield a total weight of 5.5 g. The mixture was poured into 100 mm petri dishes (639160, Greiner Bio-One, Monroe, NC, USA), which served as molds, degassed under a vacuum for 10 min, and cured at 65°C for 2 h. The membranes were then removed from the dishes, cut into $8 \times 8 \times 0.1$ cm pieces and stored in petri dishes until further use. All membranes were sterilized with 75% alcohol for 30 min before further use.

Compression device

The compression device comprised a DC-12V-6A power supply (MRL, Taiwan), programmable controller (FBs-PLC; Fatek, New Taipei City, Taiwan), pinch valves (T237574; Emerson, St. Louis, MO, USA), and a compression unit (Figure 1(a)). From the base, the compression unit comprised the bottom parts (Figure 1(b)), a PDMS membrane, and 12 apical parts (Figure 1(c)) that provided external compression via nitrogen gas from a gas cylinder with a mounted gas flow meter and manometer. Every apical part contained eight chambers arranged in a row; each chamber was connected to the next with Teflon tubes (Figure 1(d)), and the first chamber was connected to the nitrogen gas cylinder. The bottom parts featured wells in a 12×8 grid, similar to a 96-well plate. Chondrocytes cultured within C/G/GP hydrogel were seeded in the bottom part wells and covered with the PDMS membrane, after which the apical parts were mounted on the PDMS membrane using locking screws. To generate compressive stress, the nitrogen gas cylinder was turned on at a set gas pressure and flow rate, thus allowing gas to flow into the apical parts and pressed on the underlying PDMS membrane. The resulting PDMS membrane deformation directly compressed the C/G/GP-embedded chondrocytes to provide compressive stress. Pressure was relieved as the gas traveled from one chamber to the subsequent chamber; this increased the gas volume but decreased the gas pressure in the subsequent chamber, allowing us to examine different magnitudes of compression in a single experiment. The pinch valves were controlled by

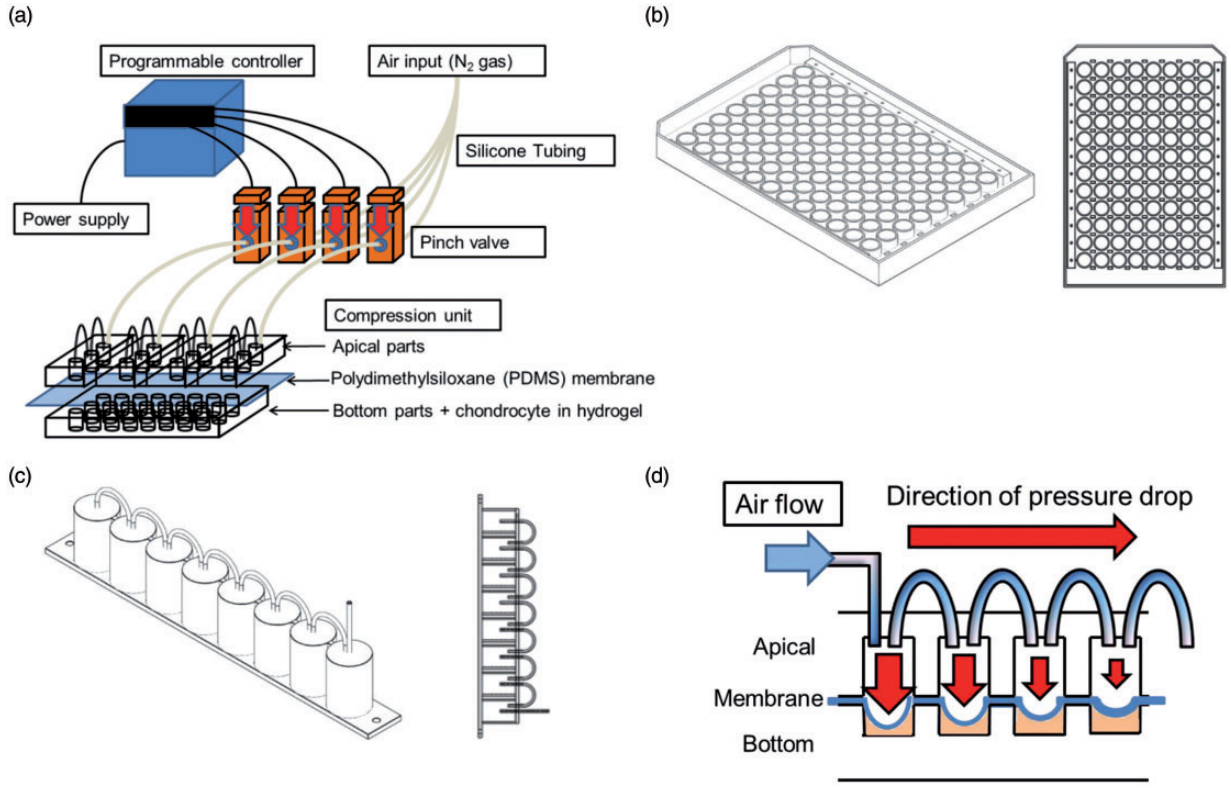

Figure 1 Compression device. (a) Device components. (b) Bottom parts of the compression unit. (c) Apical parts of the compression unit. (d) Mechanism of the compression unit. (A color version of this figure is available in the online journal.)

a programmable controller and were connected to the gas line (Figure 1(a)), thus allowing us to release or stop the nitrogen gas flow into the compression unit and generate cyclic or static loading on chondrocytes in the bottom part wells.

Induction of compressive stress

C/G/GP hydrogel was added to the bottom part wells (200 μL/well). Chondrocytes (2×10^5 cells/well) were then added to these wells and cultured at 37°C. After 24 h of incubation, the wells were covered with a PDMS membrane and then mounted under the apical parts. Compressive stress was generated using nitrogen gas at pressures of 120, 60, 40, 30, 24, 20, and 17 psi, according to the pressure drop pattern. The pressure in each chamber was estimated using equation (1)

$$P_{chamber} = \frac{P_{gas\ input} \times V_{gas\ input}}{V_{chamber(s)}} \quad (1)$$

Chondrocytes treated with constant compression for 24 h were used as the static loading group. Chondrocytes compressed at a frequency of 0.33 Hz for 24 h were designated the cyclic loading group. Chondrocytes seeded in hydrogel and placed in the compression device without treatment were used as the control group.

Chondrocyte RNA extraction and gene expression analysis

Total RNA was extracted from chondrocytes using the RNeasy Protect Mini kit (74104; QIAGEN, Hilden, Germany). First-strand complementary DNA (cDNA) was synthesized from RNA using the SuperScriptTM III First-Strand Synthesis System (18080-051; Thermo Fisher Scientific, Waltham, MA, USA) according to the manufacturer's instructions. Each single PCR was performed in a 20 μL volume containing 1 μL of primer solution, 9 μL of cDNA, and 10 μL of 2× TaqMan Universal PCR Master Mix (4304437; Thermo Fisher Scientific). The genes targeted by quantitative reverse transcription PCR (RT-qPCR) are summarized in Table 1. All PCRs were performed on an ABI PRISM 7900HT Sequence Detection System with Sequence Detection Software 2.2.2 (Applied Biosystems, Inc., Foster City, CA, USA). Target gene expression values were normalized to glyceraldehyde-3-phosphate dehydrogenase (GAPDH) expression values. The relative mRNA expression of each target gene was determined using the ΔΔCt method.

BMP-7 protein concentration analysis

After compression, BMP-7 protein was detected in chondrocytes using the Porcine BMP-7 ELISA kit (106211; Genorise Scientific, Berwyn, PA, USA) per the manufacturer's protocol.

Table 1 Primers of real-time PCR

Target gene	Assay ID	GeneBank accession number
GAPDH	Ss03375435_u1	AF141959.1
COLLAGEN I	Ss03375690_u1	AJ289757.1
COLLAGEN II	Ss03373344_g1	AF201724.1
AGGRECAN	Ss03374824_g1	X60107.1
MMP-13	Ss03373279_m1	AF069643.1
TIMP-1	Ss03381944_u1	S96211.1
IL-6	Ss03384604_ul	AB194100.1

Analysis of sulphated glycosaminoglycan content

Sulphated glycosaminoglycan (GAG) production was evaluated using a dimethylmethylene blue (DMMB, 341088; Sigma) assay, as previously described.[18] After the 24-h compression period, cells were reseeded into 6-well cell culture plates and incubated for three days. Culture medium was collected from each sample, and 40 μL aliquots were transferred to a 96-well microplate; subsequently, 250 μL of DMMB solution was added to each well. DMMB-sulphated GAG complexes were examined using an ELISA reader at a wavelength of 595 nm. The sulphated GAG content of each sample was determined using a chondroitin-6-sulphate (C4384; Sigma) calibration curve. The sulphated GAG production was normalized according to cell numbers using a total DNA assay (sulphated GAG to DNA ratio).

Alcian blue staining

After a 24-h compression, cells were reseeded into 4-well chamber-slides and cultured for three days. Chondrocytes were washed twice with PBS, fixed in 10% neutral buffered formalin (H121-08; Mallinckrodt Pharmaceuticals, St. Louis, MO, USA) for 30 min, and washed twice with PBS. Alcian blue (pH 1.0; Muto Pure Chemicals, Tokyo, Japan) was added to the wells for 30 min, after which cells were then washed under running water for 1 min. Nuclear fast red (1001210500; Merck, Kenilworth, NJ, USA) was added to the wells for 5 min, followed by a 1-min wash in running water. The cells were dehydrated via incubation in two changes of 95% alcohol and absolute alcohol (459844; Sigma) for 1 min each.

Analysis of ROS production

ROS production was evaluated using the Total ROS/Superoxide Detection Kit (ENZ-51010; Enzo Life Sciences, Farmingdale, NY, USA). After a 24-h compression, chondrocytes were collected, washed twice with PBS, and stained with 500 μL of ROS/Superoxide detection mix for 30 min in the dark. Stained samples were analyzed by flow cytometry (FC500; Beckman Coulter, Brea, CA, USA).

Statistical analysis

All data were assessed via a normality test and an equal variance test prior to the statistical analysis. Statistically significant differences between groups were determined using a one-way repeated measures analysis of variance (ANOVA). Results are expressed as means ± standard deviations of the means (SDs), and differences were considered significant at $P < 0.05$. SigmaPlot version 12.3 software (Systat Software Inc., San Jose, CA, USA) was used for all statistical analyses.

Results

Expression of ECM-related genes in response to static or cyclic loading

As described in the Methods section, chondrocytes were designated into static and cyclic groups depending on whether they were subjected to static or cyclic loading, respectively. Normalized fold-changes in gene expression were compared to the expression levels in fresh chondrocytes (control group), which were set to 1.

As shown in Figure 2(a), type I collagen gene expression in the static group increased significantly as pressure increased from 20 to 60 psi, and peaked at 24 psi with a 3.43-fold change relative to the control (20 psi, $P = 0.003$; 24–60 psi, $P < 0.001$). Type II collagen gene expression decreased significantly from 40 to 120 psi relative to the control (40–120 psi, $P < 0.001$). Aggrecan expression decreased markedly from 17 to 120 psi relative to the control (17 psi, $P = 0.048$; 20 psi, $P = 0.029$; 24 psi, $P = 0.010$; 30–120 psi, $P < 0.001$). As shown in Figure 2(b), type I collagen expression was significantly upregulated in the cyclic group from 30 to 120 psi, peaking at 30 psi with a 1.45-fold difference relative to the control (30 psi, $P = 0.002$; 40 psi, $P = 0.020$; 60 psi, $P = 0.013$; 120 psi, $P = 0.007$). Type II collagen expression increased significantly from 30 to 60 psi and peaked at 30 psi, with a 1.49-fold difference relative to the control (30 psi, $P = 0.003$; 40 psi, $P = 0.007$; 60 psi, $P = 0.044$). Aggrecan expression increased markedly from 24 to 60 psi and reached a peak at 40 psi, with a 2.04-fold difference relative to the control (24 psi, $P = 0.047$; 30 psi and 40 psi, $P < 0.001$; 60 psi, $P = 0.017$).

MMP-13 and TIMP-1 expression following static or cyclic loading

As shown in Figure 3(a), MMP-13 expression was upregulated in the static group after compression at pressures of 40–60 psi and peaked at 60 psi, with a 2.13-fold difference relative to the control (40 psi, $P = 0.006$; 60 psi, $P < 0.001$). TIMP-1 expression increased significantly from 40 to 120 psi and peaked at 120 psi, with a 2.70-fold difference relative to the control (40–120 psi, $P < 0.001$). As shown in Figure 3(b), no significant differences in MMP-13 and TIMP-1 expression were observed in the cyclic group relative to the control group at any compression pressure.

IL-6 expression with static or cyclic loading

As shown in Figure 4, IL-6 expression in the static group increased from 30 to 120 psi and peaked at 120 psi, with a 2.50-fold difference relative to the control (30–120 psi, $P < 0.001$). In the cyclic group, no significant differences were observed in IL-6 expression relative to the control group except at a compression pressure of 120 psi ($P = 0.002$).

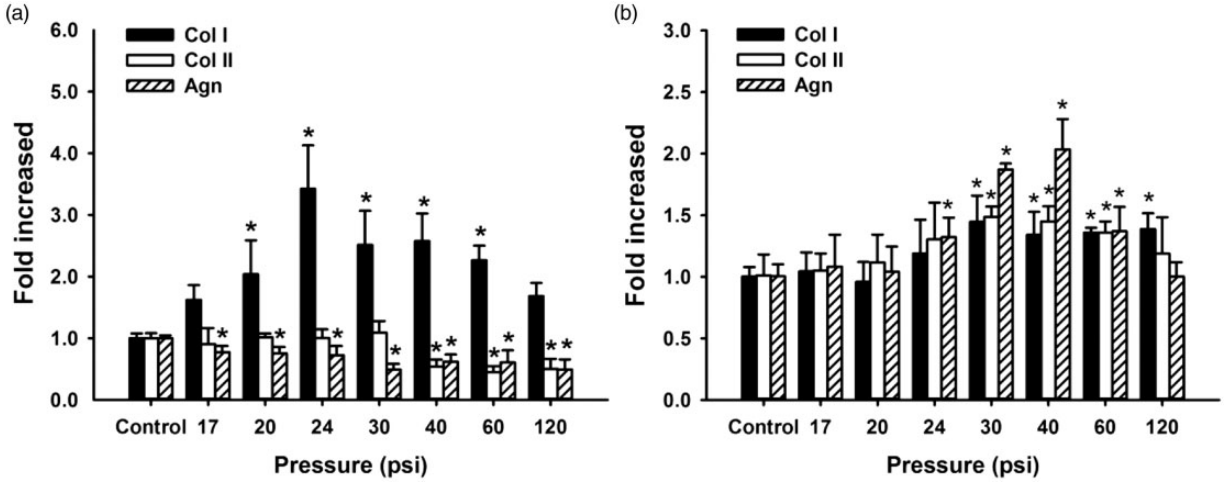

Figure 2 Expression of extracellular matrix (ECM)-related genes in chondrocytes. The expression levels of genes encoding type I collagen, type II collagen, and aggrecan are shown. Chondrocytes were stimulated with (a) static loading or (b) cyclic loading ranging from 17 to 120 psi for 24 h ($n = 5$; five independent experiments were conducted in triplicate). Results are expressed as mRNA fold-increases relative to expression levels in normal chondrocytes. Expression of each target gene was normalized to GAPDH mRNA. *$P < 0.05$, compared with the control

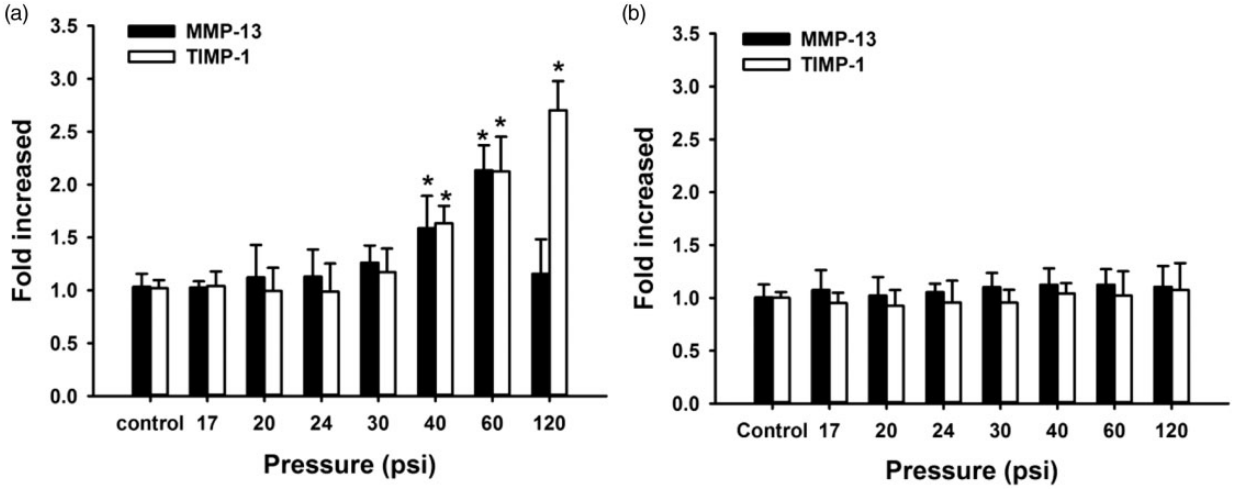

Figure 3 Expression of catabolic and anti-catabolic genes in chondrocytes. Expression levels of the genes encoding MMP-13 and TIMP-1 are shown. Chondrocytes were stimulated with (a) static loading or (b) cyclic loading ranging from 17 to 120 psi for 24 h ($n = 5$; five independent experiments were conducted in triplicate). The results are expressed as mRNA fold-increases relative to normal chondrocytes. Each target gene was normalized to GAPDH mRNA. *$P < 0.05$, compared with the control

TGF-β_1 expression and BMP-7 protein expression with static or cyclic loading

As shown in Figure 5(a), TGF-β_1 gene expression in the static group increased from 24 to 120 psi and peaked at 120 psi, with a 1.81-fold difference relative to the control (24 psi, $P = 0.035$; 30 psi, $P = 0.048$; 40 psi, $P = 0.018$; 60 psi and 120 psi, $P < 0.001$). In the cyclic group, no significant differences in TGF-β_1 expression were observed relative to the control group at any pressure. As shown in Figure 5(b), no significant differences in BMP-7 production were observed in the static group relative to the control group. However, the BMP-7 protein concentration in the cyclic group significantly increased from 30 to 60 psi and peaked at 40 psi after cyclic loading (30 psi, $P = 0.032$; 40 psi, $P = 0.010$; 60 psi, $P = 0.047$).

Sulphated GAG production and alcian blue staining with static or cyclic loading

As shown in Figure 6(a), the sulphated GAG to DNA ratio in the static group gradually and significantly decreased from 24 to 120 psi relative to the control group (24–120 psi, $P < 0.001$). However, in the cyclic group, the ratio increased significantly from 20 to 40 psi (20 psi, $P = 0.041$; 24 psi, $P = 0.006$; 30 psi, $P = 0.010$; 40 psi, $P < 0.001$) but decreased at 120 psi relative to the control (120 psi, $P = 0.004$). As shown in Figure 6(b) and (c), positive alcian blue staining was observed in the control and cyclic groups, especially at approximate pressures of 24–40 psi ($P < 0.001$). Conversely, the static group exhibited markedly few blue-stained areas from 30 to 120 psi in comparison with the control group (30 psi, $P = 0.024$; 40 psi, $P = 0.001$; 60 psi

and 120 psi, $P < 0.001$). These results indicated increased production of sulphated GAGs in the ECM of the cyclic and control groups.

ROS production with static or cyclic loading

ROS production was analyzed using flow cytometry. The 490/525 nm filter set was used to detect ROS, including hydrogen peroxide (H_2O_2), peroxynitrite (ONOO−), hydroxyl radicals (HO•), nitric oxide (NO), and the peroxy radical (ROO•) (Figure 7(a) and (b), FL 1, quadrants 2 + 4). The 550/620 nm filter set was used to detect superoxide (O2•−) (Figure 7(a) and (b), FL 3, quadrants 1 + 2). Total ROS production was evaluated by combining the frequencies of FL1- and FL3-positive cells (quadrant 1 + 2 + 3). In response to an increase in compressive pressure from 24 to 120 psi, total ROS production increased significantly in the static group relative to the control group, whereas the cyclic group exhibited similar results as the control until the pressure exceeded 40 psi (Figure 7(c)).

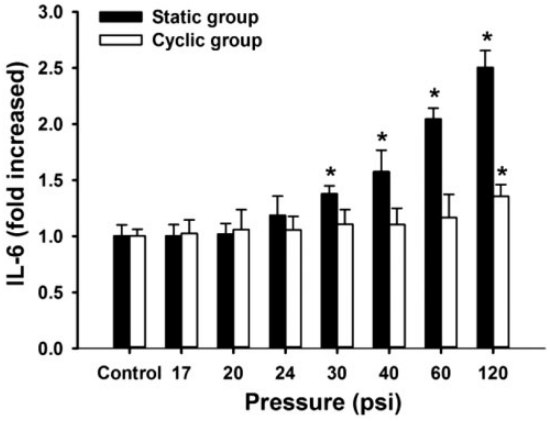

Figure 4 Expression of proinflammatory genes in chondrocytes. Expression of the gene encoding IL-6 is shown. Chondrocytes were stimulated with static loading or cyclic loading ranging from 17 to 120 psi for 24 h ($n = 5$; five independent experiments were conducted in triplicate). Results are expressed as mRNA fold-increases relative to normal chondrocytes. The target gene was normalized to GAPDH mRNA. *$P < 0.05$, compared with the control

Discussion

A moderate level of cyclic mechanical stimulus increases the production of cartilage ECM components and promotes cartilage thickening,[25,26] whereas high levels of mechanical loading induce inflammatory responses, accelerate cartilage degradation, and eventually lead to OA.[27–29] In this study, expression of the genes encoding aggrecan and type I and type II collagens were upregulated at cyclic loads of 30–40 psi, but downregulated at 60 and 120 psi (Figure 2(a) and (b)). This might indicate that although frequent dynamic loading appears to promote ECM synthesis, this phenomenon is based on the premise that loading is within a moderate range (i.e. below 60 psi). In addition, type I collagen is a major component of fibrocartilage, which lacks the biomechanical characteristics to withstand compressive stresses distributed across the knee; furthermore, elevated levels of type I collagen mRNA have been observed in osteoarthritic human cartilage.[30,31] Therefore, apart from the trend of ECM synthesis, the increased levels of type I collagen mRNA implicated that sturdy ECM anabolism could only partially benefit from cyclic loading at a moderate magnitude. In contrast, we observed no significant decreases in aggrecan and type II collagen gene expression, even at the highest cyclic loading values (120 psi) (Figure 2(b)). However, aggrecan and type II collagen gene expression were significantly downregulated type I collagen gene expression was upregulated in the static group at loads exceeding 40 psi (Figure 2(a)); this is an early sign of reduced ECM synthesis, a primary event in chondrocyte degeneration.[24]

Expression of the pro-inflammatory cytokine IL-6, which is strongly elevated in OA cartilage, inhibits synthesis of the desired matrix.[32] IL-6 can contribute directly to the inhibitory effect of aggrecan via the Notch receptor and thus activate matrix metallopeptidase-13 (MMP-13), a catabolic factor for proteoglycans and type II collagen

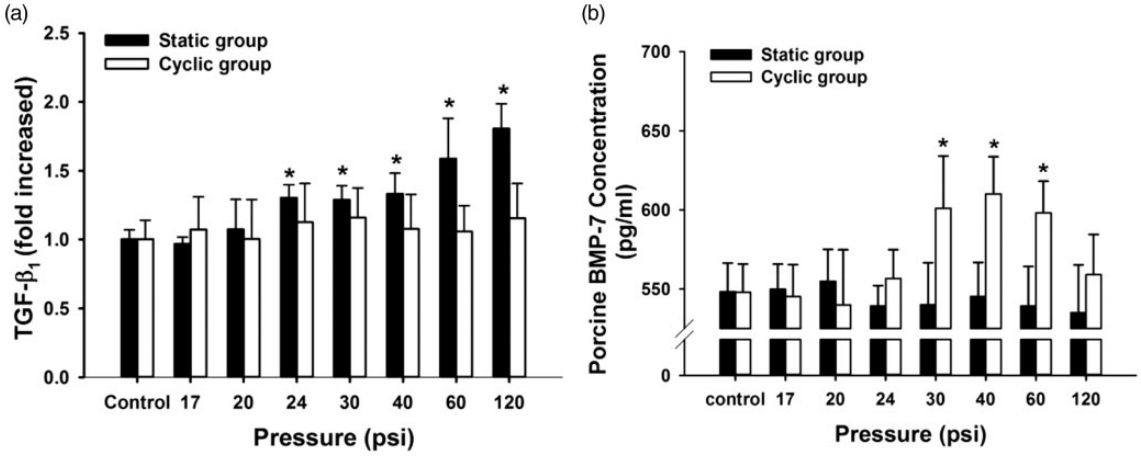

Figure 5 Expression of anabolic genes and proteins in chondrocytes. (a) TGF-β_1 gene and (b) BMP-7 protein expression are shown. Chondrocytes were stimulated with static loading or cyclic loading ranging from 17 to 120 psi for 24 h ($n = 5$ for TGF-β_1 and $n = 4$ for BMP-7; independent experiments were conducted in triplicate). Target gene expression was normalized to GAPDH mRNA. *$P < 0.05$, compared with the control

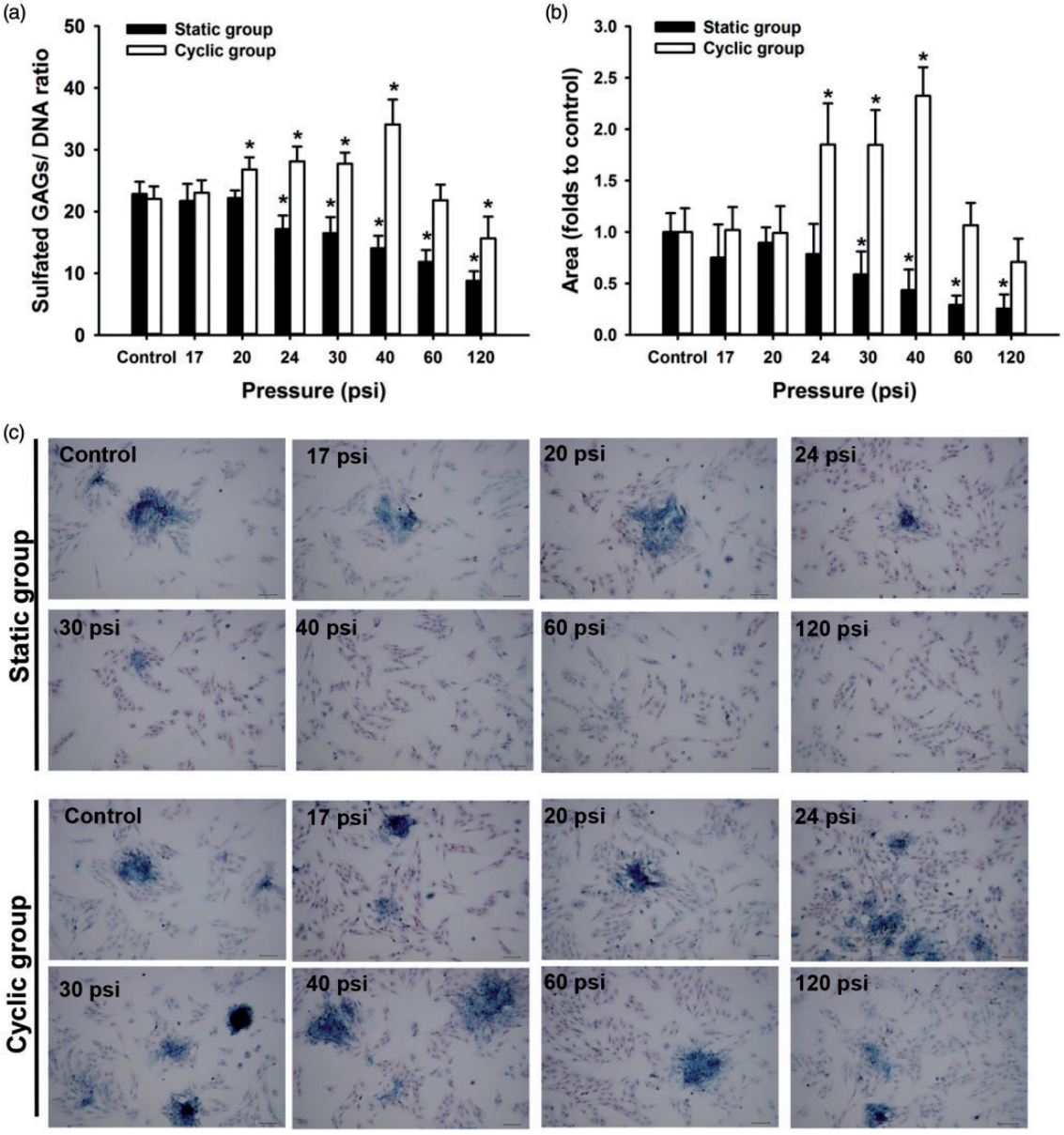

Figure 6 Sulphated-glycosaminoglycan (GAG) production after compression. (a) The ratio of sulphated GAGs to DNA in chondrocytes after static or cyclic loading (17–120 psi) for 24 h ($n = 5$; five independent experiments were conducted in triplicate). (b) Areas of alcian blue-positive extracellular matrix (ECM) after static or cyclic loading (17–120 psi) for 24 h ($n = 5$ experiments per group). (c) Alcian blue and nuclear fast red staining of static and cyclic groups under control conditions and at 17, 20, 24, 30, 40, 60, and 120 psi. Scale bar = 100 μm. *$P < 0.05$, compared with the control. (A color version of this figure is available in the online journal.)

degradation.[33–36] In contrast to MMP-13, the tissue metallopeptidase inhibitor-1 (TIMP-1) is an endogenous inhibitor of bone matrix degradation that binds tightly to active MMP-13 and thereby downregulates its activity.[37] In this study, MMP-13, TIMP-1, and IL-6 gene expression were largely unaffected (the latter was only upregulated at 120 psi of cyclic loading) (Figures 3(b) and (4)), indicating no obvious ECM degradation or inflammation at cyclic loading <120 psi and suggesting that cyclic compression has a lesser effect on OA stimulation, as demonstrated by the qPCR and GAG analysis results (Figures 2(b) and 6). In contrast, when chondrocytes were stimulated under static loading up to 40 psi, the gene expression of both IL-6 and MMP-13 was elevated in a loading-dependent manner along with reduced GAG levels (Figures 3(a), 4, and 6). Together, these features suggest the accelerated ECM catabolism observed in early OA.[24,38] Concomitant upregulation of the TIMP-1 gene confirms the induction of MMP-13 expression after static loading, and the subsequent induction of TIMP-1 expression to counteract MMP-13 (Figure 3(a)).

TGF-β_1 and BMP-7 are known anabolic factors that have been shown to increase chondrocyte proliferation and cartilage ECM production and to play critical roles in the maintenance of articular cartilage homeostasis.[39,40] Strong TGF-β_1 expression reflects the chondrocytic attempt to repair degraded ECM.[41] Additional reports indicate that ROS can stimulate TGF-β_1 expression in different types of cells,

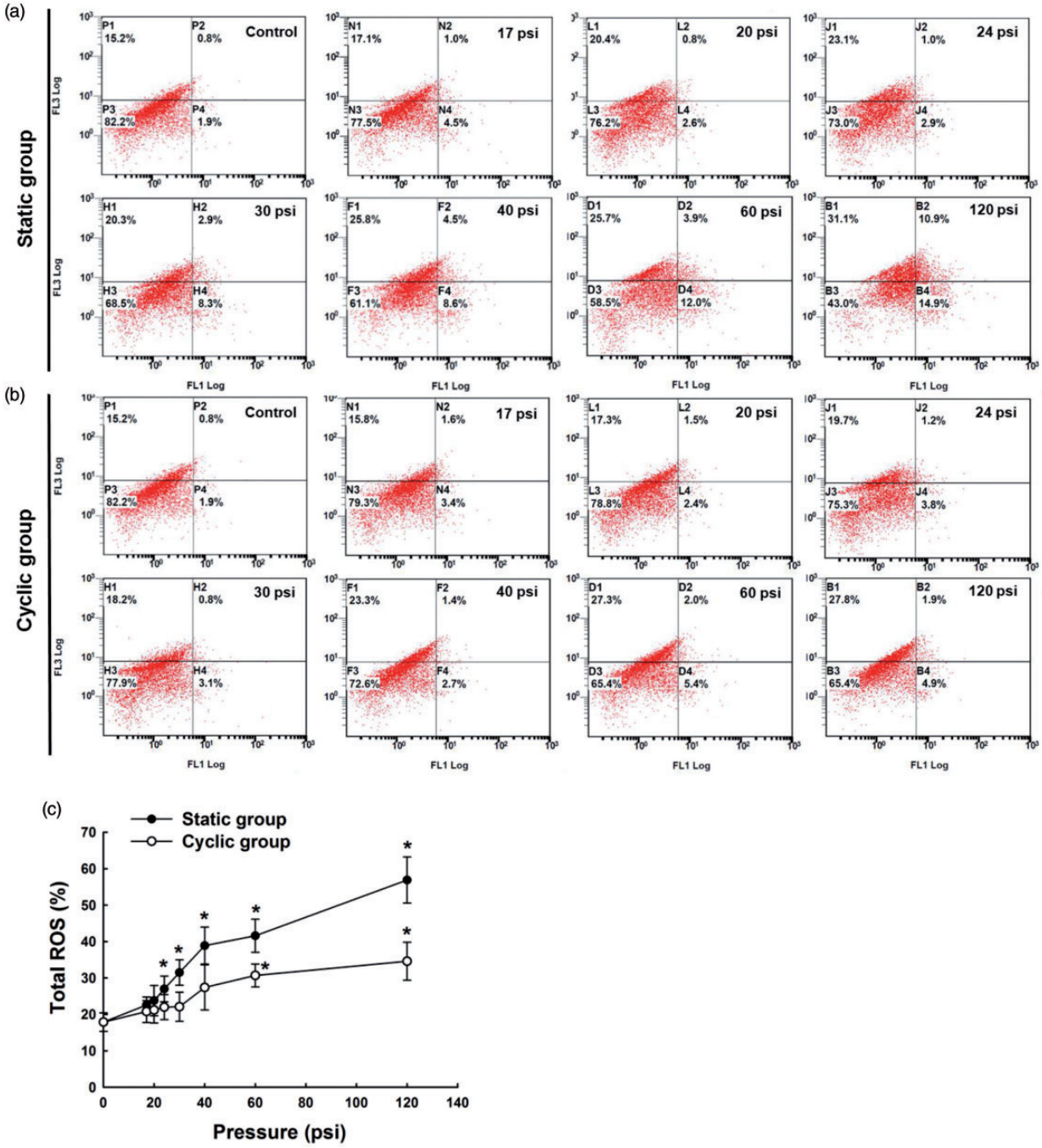

Figure 7 Reactive oxygen species (ROS) production after compression. Hydrogen peroxide, peroxynitrite, hydroxyl radicals, nitric oxide, peroxy radical (FL1), and superoxide (FL3) production were evaluated after treatment in the (a) static group and (b) cyclic group under control conditions and at 17, 20, 24, 30, 40, 60, and 120 psi. (c) Percentages of total ROS were evaluated by combining the percentages of FL1 and FL3-positive cells (quadrant 1 + 2 + 3). *$P < 0.05$, compared with the control ($n = 5$ experiments per group). (A color version of this figure is available in the online journal.)

including chondrocytes, via the activation of MMPs.[42–45] Similar results were also observed in the present study. Concomitant increases in TGF-β_1 and MMP-13 gene expression and ROS production were observed after static loading at levels above 40 psi (Figures 3(a), 5(a), and 7), indicating ECM catabolism and chondrocyte deterioration after static loading. BMP-7 has been shown to enhance the chondrogenic differentiation of progenitor cells and cartilage-specific matrix production.[46] Significantly upregulated BMP-7 gene expression has been observed in cartilage constructs exposed to dynamic biomechanical stimulation.[47] In the present study, increased BMP-7 production was observed in chondrocytes after cyclic loading (Figure 5(b)), suggesting that this type of loading may induce BMP-7 expression and further promote ECM production.

ROS were found to affect cytokine-induced MMP-13 gene expression in human articular chondrocytes.[48] In chondrocyte-related pathologies, excess ROS can damage not only the cellular membrane and nucleic acids, but also the associated extracellular matrix, resulting in cell death

and cartilage degradation.[44] In our study, ROS were elevated after static and cyclic loading, especially at high compression magnitude (Figure 7, 60–120 psi), indicating a direct correlation of ROS production with compressive stress. High compression stress renders chondrocytes at risk of increased oxidative stress.

In the normal chondrocyte, proteoglycans and type II collagen help to provide mechanical support to the cartilage. Proteoglycans comprise core proteins with attached GAGs, such as chondroitin sulphate and keratin sulphate.[5,6] In the degenerated cartilage, a decrease in chondroitin sulphate results in a decrease in water, thus attenuating the ability of cartilage to sustain external stresses.[8] In this study, the sulphated GAG to DNA ratio decreased significantly in response to static loading (Figure 6(a)). However, moderate (30–40 psi) cyclic loading significantly increased the production of ECM components. Positive alcian blue staining demonstrated the presence of sulphated GAGs in the cyclic group (Figure 6(c)). The results reaffirm that moderate and cyclic compression stress can contribute to chondrocyte ECM synthesis, whereas heavy compression will reduce ECM production.

Conclusion

In conclusion, this study demonstrated that in chondrocytes, moderate cyclic compression can promote ECM synthesis and increased GAG production. In contrast, chondrocytes subjected to static loading exceeding 40 psi for 24 h exhibited signs of decreased ECM anabolism, increased ECM degradation, and increased oxidative stress, which are the primary signs of OA. Therefore, static loading is considered more likely than cyclic loading to promote the induction of OA-like chondrocytes. For induction, 60 psi of static loading is sufficient to induce porcine chondrocytes to exhibit signs of OA, and this load will be used to generate an OA-like disease model for future compound screening studies. We suggest that this cell-based OA-like system could be generated using specific magnitudes of static loading and exhibits potential as a disease model for early-stage screening.

Authors' contributions: ICY, AG, CHH, and FHL conceived the research. ICY and CHH designed this work. CHH and FHL contributed new reagents and analytical tools. ICY performed the experiment. ICY, STC, WTK, and CTY analyzed data. ICY, STC, and FHL wrote the manuscript. ICY, STC, AG, WTK, CTY, CHH, and FHL approved the final version of the manuscript.

ACKNOWLEDGMENTS

This study was financially supported by National Science Council grant No. 100-2313-B-002-049-MY2.

DECLARATION OF CONFLICTING INTERESTS

The author(s) declare no potential conflicts of interest related to the research, authorship, and/or publication of this article.

REFERENCES

1. Huang TL, Wu CC, Yue J, Sumi S, Yang KC. l-Lysine regulates tumor necrosis factor-alpha and matrix metalloproteinase-3 expression in human osteoarthritic chondrocytes. *Process Biochem* 2016;**51**:904–11
2. Neogi T, Zhang Y. Epidemiology of osteoarthritis. *Rheum Dis Clin North Am* 2013;**39**:1–19
3. Guilak F. Biomechanical factors in osteoarthritis. *Best Pract Res Clin Rheumatol* 2011;**25**:815–23
4. Calamia V, Mateos J, Fernández-Puente P, Lourido L, Rocha B, Fernández-Costa C, Montell E, Vergés J, Ruiz-Romero C, Blanco FJ. A pharmacoproteomic study confirms the synergistic effect of chondroitin sulfate and glucosamine. *Sci Rep* 2014;**4**:5069
5. Chen WC, Wei YH, Huang JB, Chu IM, Yao CL. Biological effects of oligosaccharide chondroitin sulfate C on human articular chondrocytes. *Biomed Eng Appl Basis Commun* 2011;**23**:245–52
6. Clouet J, Vinatier C, Merceron C, Pot-vaucel M, Maugars Y, Weiss P, Grimandi G, Guicheux J. From osteoarthritis treatments to future regenerative therapies for cartilage. *Drug Discov Today* 2009;**14**:913–25
7. Natoli RM, Athanasiou KA. Traumatic loading of articular cartilage: Mechanical and biological responses and post-injury treatment. *Biorheology* 2009;**46**:451–85
8. Sellam J, Berenbaum F. Osteoarthritis and obesity. *Rev Prat* 2012;**62**:621–4
9. Kurz B, Lemke A, Kehn M, Domm C, Patwari P, Frank EH, Grodzinsky AJ, Schünke M. Influence of tissue maturation and antioxidants on the apoptotic response of articular cartilage after injurious compression. *Arthritis Rheum* 2004;**50**:123–30
10. Lepetsos P, Papavassiliou AG. ROS/oxidative stress signaling in osteoarthritis. *Biochim Biophys Acta* 2016;**1862**:576–91
11. Li D, Xie G, Wang W. Reactive oxygen species: the 2-edged sword of osteoarthritis. *Am J Med Sci* 2012;**344**:486–90
12. Yamazaki K, Fukuda K, Matsukawa M, Hara F, Matsushita T, Yamamoto N, Yoshida K, Munakata H, Hamanishi C. Cyclic tensile stretch loaded on bovine chondrocytes causes depolymerization of hyaluronan: involvement of reactive oxygen species. *Arthritis Rheum* 2003;**48**:3151–8
13. Fang HW. Trends and challenges of cartilage tissue engineering. *Biomed Eng Appl Basis Commun* 2009;**21**:149–55
14. Orth P, Rey-Rico A, Venkatesan JK, Madry H, Cucchiarini M. Current perspectives in stem cell research for knee cartilage repair. *Stem Cells Cloning* 2014;**7**:1–17
15. Thysen S, Luyten FP, Lories RJ. Targets, models and challenges in osteoarthritis research. *Dis Model Mech* 2015;**8**:17–30
16. Guingamp C, Gegout-Pottie P, Philippe L, Terlain B, Netter P, Gillet P. Mono-iodoacetate-induced experimental osteoarthritis: a dose-response study of loss of mobility, morphology, and biochemistry. *Arthritis Rheum* 1997;**40**:1670–9
17. van Buul GM, Siebelt M, Leijs MJ, Bos PK, Waarsing JH, Kops N, Weinans H, Verhaar JA, Bernsen MR, van Osch GJ. Mesenchymal stem cells reduce pain but not degenerative changes in a mono-iodoacetate rat model of osteoarthritis. *J Orthop Res* 2014;**32**:1167–74
18. Patil D, Dhaneshwar S, Kadam P. Diacerein-thymol prodrug: in vivo release and pharmacological screening in experimental models of osteoarthritis in Wistar rats. *Inflamm Allergy Drug Targets* 2015;**13**:393–405.
19. Ma Z, Piao T, Wang Y, Liu J. Astragalin inhibits IL-1β-induced inflammatory mediators production in human osteoarthritis chondrocyte by inhibiting NF-κB and MAPK activation. *Int Immunopharmacol* 2015;**25**:83–7
20. Xu J, Zhang C. In vitro isolation and cultivation of human chondrocytes for osteoarthritis renovation. *In Vitro Cell Dev Biol Anim* 2014;**50**:623–9
21. Yang F, Patterson RP. A simulation study on the effect of thoracic conductivity inhomogeneities on sensitivity distributions. *Ann Biomed Eng* 2008;**36**:762–8
22. Nicodemus GD, Bryant SJ. Mechanical loading regimes affect the anabolic and catabolic activities by chondrocytes encapsulated in PEG hydrogels. *Osteoarthritis Cartilage* 2010;**18**:126–37

23. Zhang K, Wang L, Han Q, Heng BC, Yang Z, Ge Z. Relationship between cell function and initial cell seeding density of primary porcine chondrocytes in vitro. *Biomed Eng Appl Basis Commun* 2013;**25**:1340001
24. Cheng YH, Yang SH, Lin FH. Thermosensitive chitosan-gelatin-glycerol phosphate hydrogel as a controlled release system of ferulic acid for nucleus pulposus regeneration. *Biomaterials* 2011;**32**:6953–61
25. Bader DL, Salter DM, Chowdhury TT. Biomechanical influence of cartilage homeostasis in health and disease. *Arthritis* 2011;**2011**:979032
26. Juhász T, Matta C, Somogyi C, Katona É, Takács R, Soha RF, Szabó IA, Cserháti C, Szódy R, Karácsonyi Z, Bakó E, Gergely P, Zákány R. Mechanical loading stimulates chondrogenesis via the PKA/CREB-Sox9 and PP2A pathways in chicken micromass cultures. *Cell Signal* 2014;**26**:468–82
27. Hill CL, Seo GS, Gale D, Totterman S, Gale ME, Felson DT. Cruciate ligament integrity in osteoarthritis of the knee. *Arthritis Rheum* 2005;**52**:794–9
28. Li Y, Frank EH, Wang Y, Chubinskaya S, Huang HH, Grodzinsky AJ. Moderate dynamic compression inhibits pro-catabolic response of cartilage to mechanical injury, tumor necrosis factor-α and interleukin-6, but accentuates degradation above a strain threshold. *Osteoarthritis Cartilage* 2013;**21**:1933–41
29. Lohmander LS, Ostenberg A, Englund M, Roos H. High prevalence of knee osteoarthritis, pain, and functional limitations in female soccer players twelve years after anterior cruciate ligament injury. *Arthritis Rheum* 2004;**50**:3145–52
30. Martin I, Jakob M, Schäfer D, Dick W, Spagnoli G, Heberer M. Quantitative analysis of gene expression in human articular cartilage from normal and osteoarthritic joints. *Osteoarthritis Cartilage* 2001;**9**:112–8
31. Rufino AT, Ribeiro M, Sousa C, Judas F, Salgueiro L, Cavaleiro C, Mendes AF. Evaluation of the anti-inflammatory, anti-catabolic and pro-anabolic effects of E-caryophyllene, myrcene and limonene in a cell model of osteoarthritis. *Eur J Pharmacol* 2015;**750**:141–50
32. Wang P, Guan PP, Guo C, Zhu F, Konstantopoulos K, Wang ZY. Fluid shear stress-induced osteoarthritis: roles of cyclooxygenase-2 and its metabolic products in inducing the expression of proinflammatory cytokines and matrix metalloproteinases. *FASEB J* 2013;**27**:4664–77
33. Zanotti S, Canalis E. Interleukin 6 mediates selected effects of Notch in chondrocytes. *Osteoarthritis Cartilage* 2013;**21**:1766–73
34. Ashraf S, Mapp PI, Burston J, Bennett AJ, Chapman V, Walsh DA. Augmented pain behavioral responses to intra-articular injection of nerve growth factor in two animal models of osteoarthritis. *Ann Rheum Dis* 2014;**73**:1710–8
35. Enochson L, Stenberg J, Brittberg M, Lindahl A. GDF5 reduces MMP13 expression in human chondrocytes via DKK1 mediated canonical Wnt signaling inhibition. *Osteoarthritis Cartilage* 2014;**22**:566–77
36. Halbwirth F, Niculescu-Morzsa E, Zwickl H, Bauer C, Nehrer S. Mechanostimulation changes the catabolic phenotype of human dedifferentiated osteoarthritic chondrocytes. *Knee Surg Sports Traumatol Arthrosc* 2015;**23**:104–11
37. Lee YJ, Lee EB, Kwon YE, Lee JJ, Cho WS, Kim HA, Song YW. Effect of estrogen on the expression of matrix metalloproteinase (MMP)-1, MMP-3, and MMP-13 and tissue inhibitor of metalloproternase-1 in osteoarthritis chondrocytes. *Rheumatol Int* 2003;**23**:282–8
38. Troeberg L, Nagase H. Proteases involved in cartilage matrix degradation in osteoarthritis. *Biochim Biophys Acta* 2012;**1824**:133–45
39. Li TF, O'Keefe RJ, Chen D. TGF-beta signaling in chondrocytes. *Front Biosci* 2005;**10**:681–8
40. Park H, Temenoff JS, Holland TA, Tabata Y, Mikos AG. Delivery of TGF-beta1 and chondrocytes via injectable, biodegradable hydrogels for cartilage tissue engineering applications. *Biomaterials* 2005;**26**:7095–103
41. Pujol JP, Chadjichristos C, Legendre F, Bauge C, Beauchef G, Andriamanalijaona R, Galera P, Boumediene K. Interleukin-1 and transforming growth factor-beta 1 as crucial factors in osteoarthritic cartilage metabolism. *Connect Tissue Res* 2008;**49**:293–7
42. Li WQ, Qureshi HY, Liacini A, Dehnade F, Zafarullah M. Transforming growth factor Beta1 induction of tissue inhibitor of metalloproteinases 3 in articular chondrocytes is mediated by reactive oxygen species. *Free Radic Biol Med* 2004;**37**:196–207
43. Sullivan DE, Ferris M, Pociask D, Brody AR. The latent form of TGFbeta(1) is induced by TNFalpha through an ERK specific pathway and is activated by asbestos-derived reactive oxygen species in vitro and in vivo. *J Immunotoxicol* 2008;**5**:145–9
44. Zhao W, Zhao T, Chen Y, Ahokas RA, Sun Y. Oxidative stress mediates cardiac fibrosis by enhancing transforming growth factor-beta1 in hypertensive rats. *Mol Cell Biochem* 2008;**317**:43–50
45. Liu RM, Gaston Pravia KA. Oxidative stress and glutathione in TGF-beta-mediated fibrogenesis. *Free Radic Biol Med* 2010;**48**:1–15
46. Chubinskaya S, Segalite D, Pikovsky D, Hakimiyan AA, Rueger DC. Effects induced by BMPS in cultures of human articular chondrocytes: comparative studies. *Growth Factors* 2008;**26**:275–83
47. Nam J, Perera P, Rath B, Agarwal S. Dynamic regulation of bone morphogenetic proteins in engineered osteochondral constructs by biomechanical stimulation. *Tissue Eng Part A* 2013;**19**:783–92
48. Ahmad R, Sylvester J, Ahmad M, Zafarullah M. Involvement of H-Ras and reactive oxygen species in proinflammatory cytokine-induced matrix metalloproteinase-13 expression in human articular chondrocytes. *Arch Biochem Biophys* 2011;**507**:350–5

(Received August 28, 2016, Accepted February 14, 2017)